

Influence of pH on the preparation of dispersed Ag–TiO₂ nanocomposite

Ishrat Bano · R. Vasant Kumar · Abdul Hameed

Received: 12 July 2011 / Revised: 6 September 2011 / Accepted: 7 September 2011 / Published online: 27 September 2011
© Springer-Verlag 2011

Abstract In this paper, data concerning the effect of pH on the morphology of Ag–TiO₂ nanocomposite during photo-deposition of Ag on TiO₂ nanoparticles is reported. TiO₂ nanoparticles prepared by sol–gel method were coated with Ag by photodeposition from an aqueous solution of AgNO₃ at various pH levels ranging from 1 to 10 in a titania sol, under UV light. The as-prepared nanocomposite particles were characterized by UV–vis absorption spectroscopy, transmission electron microscopy (TEM), X-ray diffraction (XRD), and N₂ adsorption/desorption method at liquid nitrogen temperature (–196 °C) from Brunauer–Emmett–Teller (BET) measurements. It is shown that at a Ag loading of 1.25 wt.% on TiO₂, a high-surface area nanocomposite morphology corresponding to an average of one Ag nanoparticle per titania nanoparticle was achieved. The diameter of the titania crystallites/particles were in the range of 10–20 nm while the size of Ag particles attached to the larger titania particles were 3±1 nm as deduced from crystallite size by XRD and particle size by TEM. Ag recovery by photo harvesting from the solution was nearly 100%. TEM micrographs revealed that Ag-coated TiO₂ nanoparticles showed a sharp increase in the degree of agglomeration for nanocomposites prepared at basic pH values, with a corresponding sharp decrease in BET surface area especially at pH>9. The BET surface area of the Ag–TiO₂ nanoparticles was nearly constant at around

a value of 140 m² g⁻¹ at all pH from 1–8 with an anomalous maximum of 164 m² g⁻¹ when prepared from a sol at pH of 4, and a sharp decrease to 78 m² g⁻¹ at pH of 10.

Keywords Ag deposition · Photodegradation · Nanocomposite

Introduction

Major efforts in modern materials chemistry are currently being devoted to the design and fabrication of nanostructured systems with tuneable physical and chemical properties for advanced catalytic applications. Recent discoveries relating to improved properties obtainable by combining different nanostructured materials, have led to focused research towards potential of noble metal/semiconductor oxide nanocomposites in catalysis [1]. Although it has been found that many semiconductors can be used as photocatalyst, but still titanium dioxide (TiO₂) is one of the most popular oxide semiconductor material due to its availability, stability, non-toxicity, and low cost [2]. TiO₂ has a wide band gap of 3.1 and 3.2 eV for anatase and rutile, respectively, which makes this material transparent to visible light, i.e., no photon absorption occurs at wavelengths greater than 380 nm and photocatalytic reactions using pure TiO₂ must be carried out using ultraviolet photons [3]. The photo generated electron and hole pairs are liable to recombination, leading to low quantum yields [4].

To improve the photocatalytic response of TiO₂ by enhancing the separation of electron–hole pairs, numerous methods including doped and composite structures, such as transition metal-based NiO, Fe³⁺, and Ni²⁺ [5–7] or non-metal-based nitrogen, polyethylene glycol (PEG), n-TiO₂,

I. Bano (✉) · R. V. Kumar
Department of Materials Science and Metallurgy,
University of Cambridge,
Cambridge CB2 3QZ, UK
e-mail: ib296@yahoo.co.uk

A. Hameed
Department of Microbiology, Quaid-I-Azam University,
Islamabad 45320, Pakistan

sulfur, and carbon [8–11] doped TiO₂ and dye (methyl orange, formaldehyde, rhodamine B (RhB)) [3, 12] or metal complex (2,2'-bipyridine, 4,4'-diethylester-2, 2'-biquinoline) [13] sensitized TiO₂ have been developed. So far, it has been shown by many researchers that the modifications of TiO₂ nanoparticles by surface impregnation with noble metals such as Au, Pt, and Ag is one successful way to improve the photocatalytic activity of TiO₂ [14–16]. A noble metal deposited on TiO₂ can play the role of mediating some of the electrons away from TiO₂ surface and preclude them from recombination with holes. Noble metal nanoparticles promote electron transfer processes and provide a way to enhance the photo efficiency of the semiconductor [17]. Among the noble metals, TiO₂ nanocomposite, Ag–TiO₂, is well known because it has strong catalytic and antibacterial abilities [16]. Surface modification of TiO₂ with noble metal like Ag has been reported to decrease the electron–hole recombination problem [18]. Ag-doped or Ag-based nanocomposites have been reported to extend photo absorption in the visible range when present in sufficient amounts.

Previous studies have also shown that the addition of silver can enhance photocatalytic activity of TiO₂. For example Kato et al. [19] reported that photodeposition of Ag on a TiO₂ film enhanced photocatalytic degradation of gaseous sulfur compounds and suggested that Ag acted as a co-catalyst. Hu et al. synthesized Ag/AgBr/TiO₂ by the deposition–precipitation method and found that it can photo degrade azodyes effectively. They also demonstrated that Ag⁰ species probably enhance the electron–hole separation and interfacial charge transfer on the surface of the catalyst [20]. Sokmen et al. [21] revealed that addition of AgNO₃ to anatase TiO₂ enhanced the photocatalytic activity and enhanced the killing of *Escherichia coli* in suspension. Kumar et al. demonstrated the synthesis of Ag–TiO₂ nanocomposite by solution impregnation method [16] and at 4 at.% loading the nanocomposite had enhanced photokilling ability in water. Hirakawa et al. synthesized Ag–TiO₂ clusters and demonstrated that the photo-induced electrons on TiO₂ can be injected into Ag core accompanying the Ag surface plasmon peak blue-shift [22]. Ag–TiO₂ particles are typically prepared by solution impregnation, deposition–precipitation, [23] sol–gel, or photodeposition method.

There has been no systematic study reporting on the effect of synthesis technique on the morphological development of Ag and TiO₂ nanoparticles. In this work, we prepared TiO₂ nanoparticles using simple sol–gel method using procedures described earlier [16], followed by photodeposition of Ag nanoparticles from aqueous AgNO₃ maintained at different pH values in the sol. An appropriate amount of NaOH or HCl was added in order to control the pH value of the AgNO₃ solution containing the titania sol. It is also aimed to find the conditions for anchoring Ag nanoparticle to TiO₂ nanoparticle and evaluate the size ratio between Ag and TiO₂

nanoparticles and the number of Ag particles per titania particle. This knowledge can be exploited for optimizing the Ag–TiO₂ nanocomposite morphology for a given photocatalytic application.

Microstructure and morphology of the nanocomposite samples were investigated by using a series of techniques such as X-ray diffraction (XRD), scanning electron microscopy (SEM), Brunauer–Emmett–Teller (BET) surface area measurements and UV–vis spectroscopy. The influence of pH on the morphology and properties is discussed.

Experimental

Materials

All chemicals were analytical grade and used without further purification. Deionized water was used as the dispersing agent through all the experiments.

Chemicals used in the synthesis were titanium isopropoxide with a purity of 97% (Aldrich, UK) as a precursor, analytical grade hydrochloric acid (HCl, 37%, Fisher, UK) as a catalyst for the peptization, and deionized water as dispersing media, PEG with an average molecular weight of 6 kg mol⁻¹ (Fluka, Germany), and AgNO₃, 99.99%(Sigma Aldrich, UK).

Method

The Ag–TiO₂ nanoparticles were prepared by a photodeposition process. TiO₂ used in this experiment were synthesized by sol–gel process by hydrolysis of titanium isopropoxide (Ti (OC₃H₇)₄, Sigma Aldrich) followed by calcination at 450 C for 2 h. One gram of TiO₂ powders were dispersed in desired volume of deionized water under ultrasonic stirring for 15 min. The oxide slurry was illuminated with UV (A) light for 20 min to oxidize any possible organic carbon impurities on the TiO₂ surface.

Photodeposition was carried out by adding a calculated volume of 0.05 M aqueous AgNO₃ into the TiO₂ nanopowder sol, so as to attain an eventual 1.25 wt.% loading of Ag. This amount was found to be the optimum value based on synthesis with varying Ag loading in order to obtain a nanocomposite morphology containing on average one Ag nanoparticle anchored on the surface of one titania nanoparticle. After the AgNO₃ was uniformly dispersed and dissolved, a 15 W UV lamp with a central wavelength of 365 nm was powered on to illuminate the sol along a normal direction for 3 h while the sol was magnetically stirred. Thus the sol is fully aerated and thus can be assumed to be saturated with oxygen. In order to vary the pH value of the solution from 1 to 10, the pH was adjusted by adding either NaOH or HCl. The suspension was centrifuged at 12,000 rpm for 10 min and then washed

with distilled water several times to remove any impurities. Lastly, the suspensions were dried at 100 °C to obtain the sample for characterization.

The formation of colloidal Ag metal nanoparticles on TiO₂ was confirmed by XRD. A series of Ag–TiO₂ nanocomposite with a constant Ag loading of 1.25 wt.% at varying pH values were prepared. The samples were labeled as pH1, pH2, pH3....pH10, denoting the relevant pH value used during photodeposition of Ag on titania nano particles.

Characterizations

Energy dispersive X-ray spectroscopy (EDX) analysis was done for the elemental composition of the nanocomposite. X-ray diffraction pattern for the structure of powder was recorded on a Philips X'pert diffractometer equipped with a CuK α radiation source (λ 1.541, 80 Å). The process of Ag–TiO₂ nanoparticles impregnation was accurately monitored by a Perkin Elmer Lambda25 UV spectrophotometer at different pH values ranging from 1 to 10. TEM images were recorded on the JEOL 200CX, which is a 200-kV analytical transmission electron microscope/scanning electron microscope (TEM/STEM). For TEM studies the samples were prepared by placing a drop of aqueous Ag–TiO₂ nanoparticles dispersion on a piece of carbon-coated copper grid under ambient conditions.

Sample powders were also characterized for their specific surface area by using N₂ adsorption/desorption method at liquid nitrogen temperature (–196 °C) from Brunauer–Emmett–Teller equation at 77.3 K using a Micromeritics Tristar 3000 analyzer. Prior to BET measurement, powders were degassed for 24 h at 90 °C under a pressure of 0.1 Pa. To prevent any possible crystallization during outgassing, higher drying temperature was avoided.

Results and discussion

X-ray diffraction

Figure 1 shows the X-ray diffraction of pure TiO₂ nanoparticles and the (1.25 wt.%) silver-loaded TiO₂ nanocomposites. In the XRD (X-ray diffraction) pattern, a peak at $2\theta = 25.3^\circ$ matching with the (101) peak and $2\theta = 55^\circ$ corresponding to (211) peak of anatase can be observed (ICSD reference code: 03-065-5714). After photodeposition of Ag, an additional peak at 2θ near 38° arises, which can be assigned to Ag (111) planes. This Ag peak which is subsumed within the TiO₂ peaks at $2\theta = 37.8^\circ$, 38.1° , and 38.6° [16, 24, 25] gives evidence for successful photoreduction of Ag ions into metallic Ag. The ratio of peak intensity between the 38.1 and 38.6 reflections are higher in the Ag–TiO₂ nanocomposite material in comparison with the pure single phase TiO₂ peaks. Despite the relatively low concentration of Ag at 1.25 wt.% (corresponding to only 0.57 volume % arising from density difference), it is quite surprising to be able to detect the presence of Ag by XRD, suggesting presence of clusters of Ag on surface increasing XRD reflections from Ag. No other peaks of secondary phases containing Ag were detected (Fig. 1). The average crystallite sizes of titania and Ag in the sample were evaluated by the Scherrer equation applied to the XRD data: $d = k\lambda/\beta \cos\theta$, where λ is 1.54 Å corresponding to irradiation wavelength, k is a coefficient 0.9, β is the full width at half maximum of strongest line and θ is the Bragg diffraction angle at the peak maximum. The crystallite sizes (d) of TiO₂ corresponding to varying pH values is shown in Table 1. The results indicate that at all pH values of photo reduction, Ag particles are crystallized and formed in the nanometer range. The calculated crystallite sizes of TiO₂ and

Fig. 1 XRD patterns of **a** TiO₂, **b** Ag–TiO₂ nanocomposite

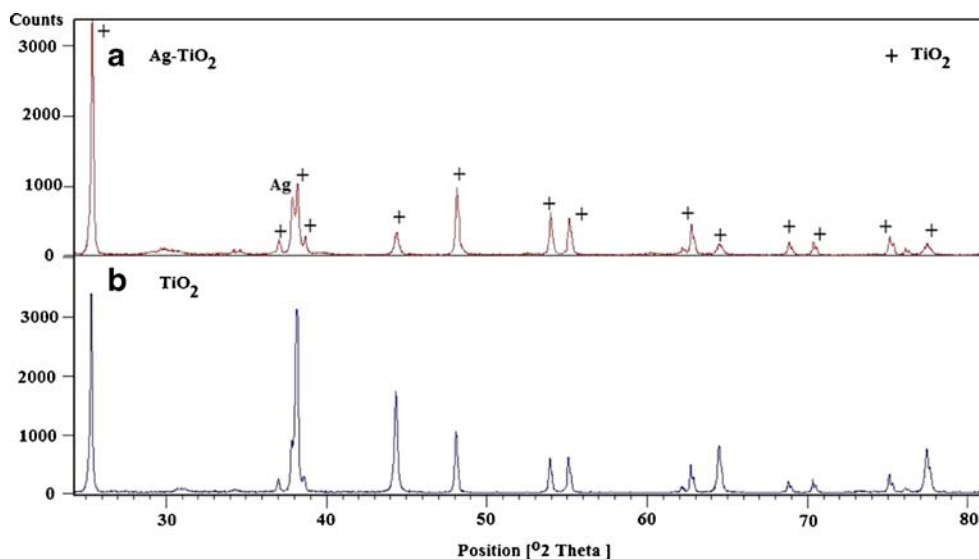


Table 1 BET surface area of Ag–TiO₂ nanocomposite, crystallite size (XRD) of TiO₂ (crystallite size of Ag remained fairly constant at 3 nm at all pH values)

Sample pH	BET surface area (m ² g ⁻¹)	Crystallite size from XRD (nm)
1	142	10
2	145	12
3	147	14
4	164	11
5	137	13
6	137	12
7	145	10
8	134	11
9	135	10
10	78	15

Ag were found to be in the range of 13±6 and 3±1 nm, respectively.

Brunauer–Emmett–Teller surface area

Table 1 shows the BET surface area data for the Ag–TiO₂ nanocomposites corresponding to the different pH values. It can be observed that the BET surface area of Ag–TiO₂ is mostly constant with increasing pH values at around 140 m² g⁻¹ with an anomalous peak of 164 m² g⁻¹ at pH 4 and then as we move towards higher pH the BET surface area decreased to 135 m² g⁻¹ at pH 9 and then at the highly alkaline pH of 10, the surface area decreased sharply to a much lower value of 78 m² g⁻¹.

It was observed that while the calculated crystallite size of TiO₂ and Ag (from XRD) did not change much with pH, the surface area decreased with increasing pH [26, 27]. The trend of decreasing surface area is due to the agglomeration of the nanocrystals as can be seen by imaging. At pH 10, a relatively steep drop in surface area shows the highest degree of agglomeration of the nanoparticles. As shown in Fig. 2, the nano pore size is more or less constant at all pH values and not affected by agglomeration.

BET Surface Area and Pore Size at Different pH Values

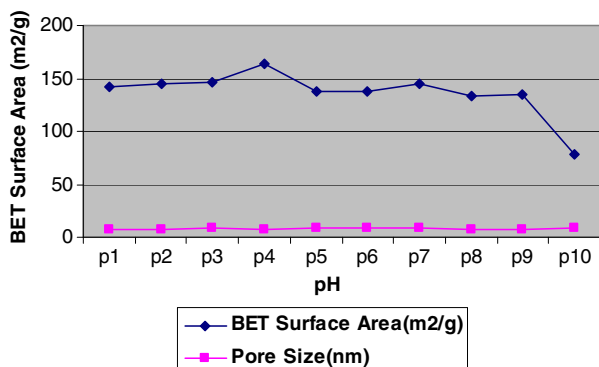


Fig. 2 BET surface area and pore size of Ag–TiO₂ nanocomposite

UV–visible spectroscopy

UV–visible absorption spectroscopy data of Ag–TiO₂ nanocomposite is displayed in Fig. 3. In this study as the concentration of Ag in the nanocomposite was very low (1.25 wt.%) and the particle size was very small and did not display any visible absorption [16, 28]. At the 1.25 wt.% loading and for the morphology observed, there was no sign of any Ag plasmon resonance. The Ag–TiO₂ nanocomposite did not show any change in the UV–vis spectra when compared with pure TiO₂ (Fig. 3). Due to the small crystallite size (3±1 nm) and the lower Ag concentration this is possibly insignificant in effect [16]. It is also obvious from the literature [23, 28] that the UV–vis absorption spectra density depends on the starting AgNO₃ concentration and absorption intensity in the visible range of the synthesized Ag–TiO₂ nanocomposite increases with the increasing AgNO₃ concentration.

Transmission electron microscope

Transmission electron microscope pattern of the Ag–TiO₂ prepared at pH 3 is presented in Fig. 4a, and the corresponding EDX spectrum from TEM is shown in Fig. 4b. The TEM result indicates that mono-dispersive

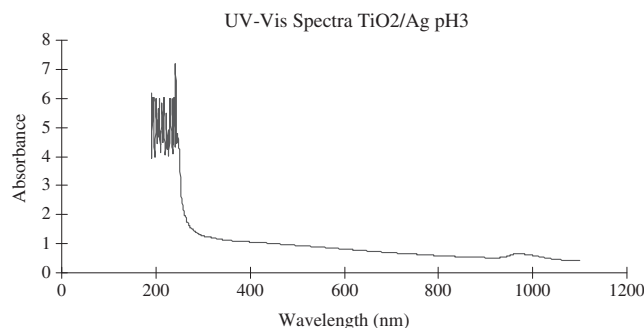


Fig. 3 UV–Vis spectra of Ag–TiO₂ photosynthesized at pH=3

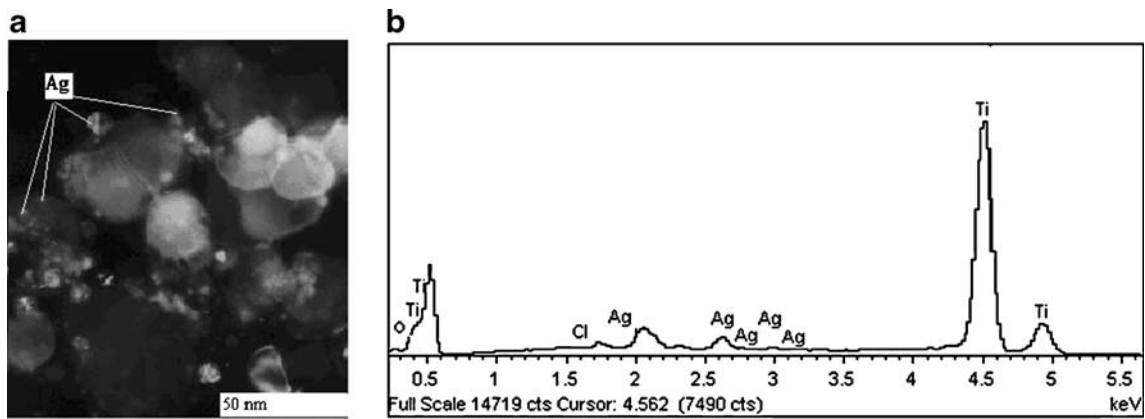


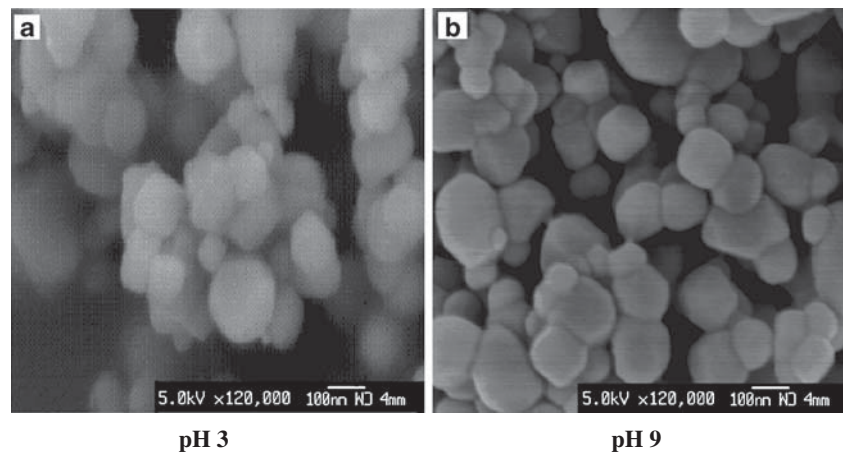
Fig. 4 **a** TEM Image of Ag–TiO₂ showing the deposits of Ag on TiO₂ nanoparticles at pH 3, **b** the corresponding EDX spectrum of Ag–TiO₂ nanocomposite at pH 3

and highly crystalline Ag–TiO₂ nanocomposite was obtained. The particles are near spherical with relatively narrow size distribution. The average particle size of primary TiO₂ and Ag nanoparticles as calculated from the TEM correspond 18±6 and 3±1 nm, respectively, which is very close to the results for the crystallite size calculated from the X-ray diffraction patterns using the Scherrer equation, with the TEM image indicating a slightly larger average primary particle size for TiO₂ in comparison with the crystal size, suggesting nanocrystals are slightly agglomerated but not greatly. The much smaller spherical Ag nanoparticle at around 3 nm is anchored on the surface a TiO₂ nanoparticle which is nearly six times larger in size. The Ag nanoparticle did not coat the TiO₂ on the whole surface but is adhered at some locations as a nanocluster such that on average we observe one Ag nanocrystal for each TiO₂ nanoparticle. From simple calculations based on the stoichiometry, and average particle size as observed, the ratio of Ag to TiO₂ is estimated at 1:1 (i.e., 1 Ag particles of 3 nm diameter for every 18 nm titania particle), in good agreement with the results from the TEM images. These

results show that Ag recovery by photo harvesting is nearly 100%. Some of the TiO₂ crystals are also seen as loosely agglomerated into large particles of 40–100 nm typically, the degree of this agglomeration relating to the value of BET surface area of a given sample. The value of pH used during photosynthesis of the composite can clearly affect the degree of agglomeration of the composite nanoparticles.

The results of EDX studies are shown in Fig. 4b, which provide additional confirmation for the presence of Ag on the surface of a TiO₂ nanoparticle. With consideration to Ag peaks which are observed in EDX pattern of Ag–TiO₂ (Fig. 5a,b) and a very small peak which was detected in XRD pattern of Ag–TiO₂ (Fig. 1), suggested the reduction to metallic silver phase on TiO₂ surface has taken place. It is clear that Ag particles with size of 3±1 nm were successfully photo deposited on the surface of TiO₂ nanoparticles (18±2 nm). The photodeposition method has led to a finer structure when compared with solution impregnation/calcinations method [16], which showed larger primary particles of Ag (≈10 nm) and TiO₂ (≈60 nm). Further

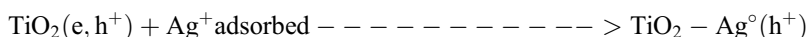
Fig. 5 **a, b** The SEM images of Ag–TiO₂ nanocomposite at pH 3 and pH 9



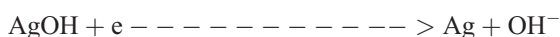
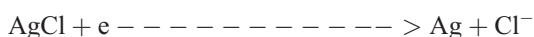
minimization of agglomeration of TiO₂ is available from control of pH.

Scanning electron microscope

Scanning electron microscope analysis of the Ag–TiO₂ nanocomposite was carried out with the aim to examine morphological changes. In SEM, the samples presented differences concerning degree of agglomeration between samples made at pH 3 and pH 9, as can be observed in Fig. 5a and b.



In water, normally holes take part in counter-oxidation reaction by oxidizing surface adsorbed water molecules into hydroxyl radical [2, 14, 22]. Since the pH in our work is controlled by the addition of HCl or NaOH, account must be taken of the relatively low solubility products of AgCl and AgOH. At a low pH (<4), AgCl and, at high pH (>9), AgOH, can be expected to be precipitated onto the TiO₂ surface which can be then assumed to be photochemically reduced to Ag under UV light. This can be described as follows



The oxidation of adsorbed water, Cl[−] or OH[−] can be expected to provide the hole scavenging reaction. The high BET surface area and the low degree of agglomeration at pH 4 and a relatively sharp decline in the BET surface area accompanied by an increase of agglomeration at pH 10 (or >9) are clearly related in some way to nucleation and growth of AgCl (at pH<4) and AgOH (at pH>9) precipitates followed by photo reduction of AgCl and AgOH. While it is clear that Ag⁺ ions from soluble AgNO₃ (aq) and from insoluble AgCl(s) or AgOH(s) can be readily photoreduced to metallic Ag on titania sol, fine tuning of agglomeration dependence on pH is available.

In summary, we have deduced the conditions under which it is possible to produce a fine nanocomposite morphology of Ag–TiO₂ such that a small- (3 nm) sized Ag particle is anchored by photodeposition onto a larger (18 nm) sized TiO₂ particle, while retaining the surface area. Using these results we are currently designing the morphological architecture of the Ag–TiO₂ nanocomposite system for optimal applications in photocatalysis, chemical sensing, and hydrogen production.

The nanocomposite produced at alkaline pH was agglomerated to a greater extent, as shown in Fig. 5b while the nanocomposites from the acidic pH, however are less agglomerated, as shown in Fig. 5a. From previous work, it is known that AgNO₃ can adsorb on the surface of TiO₂ particles in the suspension. Thus the Ag⁺ ions that are initially adsorbed on the surface of TiO₂ particles can be reduced by the photo generated electrons to silver metal atoms which tend to cluster into small nanoparticles of 3 nm (containing around 850 atoms per particle)

Conclusion

By combining results from X-ray diffraction, BET, EDX, and TEM It was found that a fine-structured Ag–TiO₂ nanocomposite with an average TiO₂ and Ag particle size 18±6 and 3±1 nm, respectively, can be produced by photodeposition of Ag in a titania sol at pH values from 1–10. At a loading of 1.25 wt.% Ag, all the Ag was photo harvested as metallic particle anchored on the surface of TiO₂, such that each TiO₂ particle is attached with one Ag particle. The N₂ adsorption–desorption isotherm showed highest BET surface area was obtained at pH 4, associated with optimal inhibition of particle agglomeration.

Acknowledgment We would like to thank UNESCO-L'Oreal Fellowship for the financial support of this project.

References

1. Zhang JZ (1997) Ultra fast studies of electron dynamics in semiconductor and metal colloidal nanoparticles: effects of size and surface. *Chem Res* 30:423–429
2. Zhao J, Yang X (2003) Photocatalytic oxidation for indoor air purification: a literature review *Build. Environ* 38:645–654
3. Zhang F, Zhao J, Shen T, Hidaka H, Pelizzetti E, Serpone N (1998) TiO₂-assisted photodegradation of dye pollutants. II. Adsorption and degradation kinetics of eosin in TiO₂ dispersions under visible light irradiation. *Appl Catal B: Environ* 15:147–156
4. Serpone N, Ezio P (1989) *Photocatalysis: fundamentals and applications*. Wiley, New York
5. Li XZ, Li FB, Yang CL, Ge WK (2001) Photocatalytic activity of WO_x-TiO₂ under visible light irradiation. *J Photochem Photobiol A* 141(2–3):209–217
6. Yu JG, Zhao XJ, Zhao QN (2000) Effect of surface structure on photocatalytic activity of TiO₂ thin films prepared by sol-gel method. *Thin Solid Films* 379(1–2):7–14
7. Ihara T, Miyoshi M et al (2003) Visible-light-active titanium oxide photocatalyst realized by an oxygen-deficient structure and by nitrogen doping. *Applied Catalysis B: Environmental* 42(4):403–409

8. Ryuhei N, Tanaka T, Nakato Y (2005) Oxygen photoevolution on a tantalum oxynitride photocatalyst under visible-light irradiation: how does water photooxidation proceed on a metal-oxynitride surface. *J Phys Chem B* 109(18):8920–8927
9. Bura C, Lou Y, Chen X (2003) *Nano Lett* 3:1049
10. Khan SUM, Al-Shahry M, Ingler WB (2002) Efficient photochemical water splitting by a chemically modified n-TiO₂. *Science* 297:2243–2245
11. Ohno T, Akiyoshi M et al (2004) Preparation of S-doped TiO₂ photocatalysts and their photocatalytic activities under visible light. *Appl Catal A: Gen* 265(1):115–121
12. Liu G, Zhao J, Hidka H et al (2000) ESR spin-trapping detection of radical intermediates in the TiO₂-assisted photooxidation of sulforhodamine B under visible irradiation. *J Photochem Photobiol A:Chem* 133:83–88
13. Hoertz PG, Thompson DW, Friedman LA, Meyer GJ (2002) Ligand localized electron trapping at sensitized semiconductor interfaces. *J Am Chem Soc* 124:9690–9691
14. Chan SC, Barteau MA (2005) Preparation of highly uniform Ag/TiO₂ and Au/TiO₂ supported nanoparticle catalysts by photodeposition. *J Langmuir* 21(12):5588–5595
15. Keller V, Bernhardt G, Garin F (2003) *J Langmuir* 21(12):5588–5595, 215
16. Kumar RV, Raza G (2009) Photocatalytic disinfection of water with Ag-TiO₂ nanocrystalline composite. *Ionics* 15(5):579–587
17. Toshima N (2000) Core/shell-structured bimetallic nanocluster catalysts for visible-light-induced electron transfer. *Pure Appl Chem* 72(1–2):317–325
18. Schmid G (ed) (1994) *Clusters and colloids. From theory to applications* (VCH, Weinheim, ISBN 3-527-29043-5, 555 Seiten, Preis: DM 248)
19. Kato S, Hirano Y, Iwata M, Sano T, Takeuchi K, Matsuzawa S (2005) Photocatalytic degradation of gaseous sulfur compounds by silver-deposited titanium dioxide. *Appl Catal B-Environ* 57:109–115
20. Chun Hu, Lan Y, Jiuhui Qu, Xuexiang Hu, Wang A (2006) Ag/AgBr/TiO₂ visible light photocatalyst for destruction of azodyes and bacteria. *J Phys Chem B* 110:4066–4072
21. S'okmen M, F Candan, Z S'umer (2001) *J. Photochem. Photobiol. A* 143 241
22. Hirakawa T, Kamat PV (2005) Charge separation and catalytic activity of Ag-TiO₂ core-shell composite clusters under UV-irradiation. *J Am Chem Soc* 127(11):3928–3934
23. Brook LA, Evans P, Foster HA, Pemble ME, Steele A, Sheel DW, Yates HM (2007) Highly bioactive silver and silver/titania composite films grown by chemical vapour deposition. *J Photochem Photobiol A Chem* 187:53–63
24. Pettibone John M, Cwiertny David M, Scherer M, Vicki H (2008) Grassian adsorption of organic acids on TiO₂ nanoparticles: effects of pH, nanoparticle size, and nanoparticle aggregation. *J Langmuir* 24(13):6659–6667
25. Rupa AV, Manikandan D et al (2007) Effect of deposition of Ag on TiO₂ nanoparticles on the photodegradation of reactive Yellow-17. *J Hazard Mater* 147(3):906–913
26. Li W, Ni C, Lin H, Huang CP, Ismat Shah S (2004) Size dependence of thermal stability of TiO₂ nanoparticles. *J App Phys* 96(11):6663–6668
27. Riboh JC, Haes AJ, McFarland AD, Yonzon CR, Van Duyne RP (2003) A nanoscale optical biosensor: real-time immunoassay in physiological buffer enabled by improved nanoparticle adhesion. *J Phys Chem B* 107(8):1772–1780
28. Sugimoto T, Zhou X (2002) Synthesis of uniform anatase TiO₂ nanoparticles by the gel-sol method: 2. Adsorption of OH⁻ ions to Ti (OH)₄ gel and TiO₂ particles. *J Colloid Interface Sci* 252(2):347–353